XMM-Newton CCF Release Note

XMM-CCF-REL-166

EPIC MOS metrology

B. Altieri

May 14, 2004

1 CCF components

Name of CCF	VALDATE (start of val. period)	EVALDATE (end of val. period)	List of Blocks changed	CAL VERSION	XSCS flag
EMOS1_LINCOORD_0017	1998-01-01 00:00:00		LINCOORD		NO
EMOS2_LINCOORD_0017	1998-01-01 00:00:00		LINCOORD		NO

2 Analysis

The MOS metrology has been revisited with SAS6.0, searching for systematics in the offsets of MOS peripherical CCDs with respect to the central CCD. For this purpose, several rich stellar fields have been used as well as one extragalactic field, for various position angles, see table 1.

The source lists of the MOSs, produced by edetect_chain, were correlated with the 2MASS catalogue for the stellar fields and with Lehmann (2001) catalogue for the Lockman Hole field. A cross-correlation radius of 5 arcsec was used, associating the nearest NIR source as the most probable counterpart of the X-ray source. The global XMM frame offset with optical is then corrected, setting the central CCD offset to zero and the offsets for each source projected in camera coordinate axis (DETX/DETY), i.e. a simple rotation of the Position Angle. The offsets are plotted in figure 1 in units of arcseconds, with one point per source.

The errors reported in figure 1 are the standard deviations divided by square root of the number of cross-correlation for each CCD. Some systematic offsets can clearly be evidenced.

The same study was performed by cross-correlating MOS sources directly with the pn source list instead of the optical catalogues and is shown in figure 2 : the same global systematics (amplitude

Target/Field	revolution	ObsId	Position Angle
OMC2/3	237	0093000101	273
OMC2/3	598	0134531601	266
OMC2/3	690	0134531701	86
Rho Ophicius	220	0111120201	98
NGC 2516	60	0113891001	261
NGC 2516	60	0113891101	261
NGC 2516	164	0126511201	100
NGC 2516	209	0134531201	182
NGC 2516	209	0134531301	182
NGC 2516	346	0134531501	100
Lockman Hole	70	0123700101	311
Lockman Hole	548	0147511801	101

Table 1: list of observations used for the refinement of MOS metrology

and direction of the shifts) can be observed, although with less statistics, confirming the fact that the offsets are real.

Note that no attempt was made to search for :

- a global field rotation, due to residual errors in the EULER PSI angle of the new BORESIGHT CCF issue 17. But there is obviously some dependence/degeneracy her between the LINCOORD offsets of the MOS peripherical CCDs and the MOS EULER PSI angles in the BORESIGHT CCF.
- rotations of individual CCDs, as they may not have been properly aligned between each other in the focal plane. The structure of the MOS LINCOORD CCFs allows for CCD-dependent rotation angles, but all these angles are left at zero since launch. Note that a rotation of 0.5 degree of one MOS peripherical CCD, would lead to 2.5 arcsec shift for a source at the central edges of the CCD, but up to 3.5 arcsec in the corners.

  So hopefully the CCDs have been aligned to better than 0.5 degree !

3 Changes

The shift with the previous values in the LINCOORD CCFs are given in table 2 in arcsec, they were converted in millimeters in the CCF itself (size of MOS pixel = 1.1 arcsec = 40 μm) and implemented in the LINCOORD CCF version 17.

MOS	CCD	DETX offset (arcsec)	DETY offset (arcsec)
1	1	0.0	0.0
	2	-0.4	1.0
	3	-1.3	-0.3
	4	0.5	-0.2
	5	1.1	0.6
	6	-1.5	-0.6
	7	-0.5	0.0
2	1	0.0	0.0
	2	-2.3	1.0
	3	-0.4	-1.1
	4	0.3	0.0
	5	1.7	-0.4
	6	0.0	0.4
	7	-2.7	0.0

Table 2: list of offsets applied on LINCOORD issue 16 for issue 17

4 Scientific Impact of this Update

This new issue of the LINCOORD CCFs shall improved slightly the MOS relative astrometry in the field-of-view, but more significantly in the common area covered by 3 CCDs: MOS1 CCD6 and MOS2 CCD2 and 7.

The improvements are illustrated on figure 3 and 4, for one observation on the OMC2/3 field. The result on MOS2 CCD7, and to a lesser extend MOS2 CCD7, are still not completely satisfactory but the relative CCD offsets are significantly reduced.

5 Estimated Scientific Quality

One way to estimate the improvement in the scientific quality is to measure the scatter in the errors of the relative offsets, from the X-ray source position with the most-probable optical counterparts, over the whole MOS field-of-view. This is shown in figures 5 and 6 with the old (v16) LINCOORD CCF and figures 7 and 8 for the new (v17) LINCOORD CCF in the form of scattter plots and histograms of the deviations in RA and DEC. For this particular observations of OMC 2/3 field with a lot of sources in the CCD 2 & 7 area, the 1σ of the distribution on the RA axis is reduced from 2.2 arcsec down to 1.2 arcsec with the new CCF .

The standard deviation of the MOS offset errors $\sim$1.0 arcsec per axis is still wider than for pn ($\sim$0.7 arcsec per axis), which is assembled on one single wafer, when comparing figure 9 (MOS1) with figure 10 (EPIC-pn), but is getting comparable. The wider distribution, i.e. the worse MOS metrology vs EPIC-pn is due to the still imperfect positioning of the peripherical CCDs, both linear offsets (investigated and corrected here) and possible individual CCD rotations (not attempted

here).

One can deduce from this analysis that with the new LINCOORD CCF, **the overall MOS relative astrometric accuracy is about 1.5 arcsec**, while closer to 1.0 arcsec for EPIC-pn. However the MOS relative astrometric accuracy could be slightly worse locally for some CCDs which could still show some residual offsets (<1 arcsec) or for CCDs having possibly a rotation with respect to the central CCD. In this case the shift will be higher towards the edges of the CCD.

6 Test procedures & results

See previous sections. SAS6.0 was used, comparing the MOS metrology accuracy of the new LINCOORD version 17 with the old version 16

7 Expected Updates

Possibly in the future, if CCD offsets are characterized to a better accuracy than the simple cross-correlation method used here, including the possible effect of CCD rotations.

8 References

Lehmann et al., 2001, A&A, 371, 833, "The ROSAT Deep Survey. VI. X-ray sources and Optical identifications of the Ultra Deep Survey"

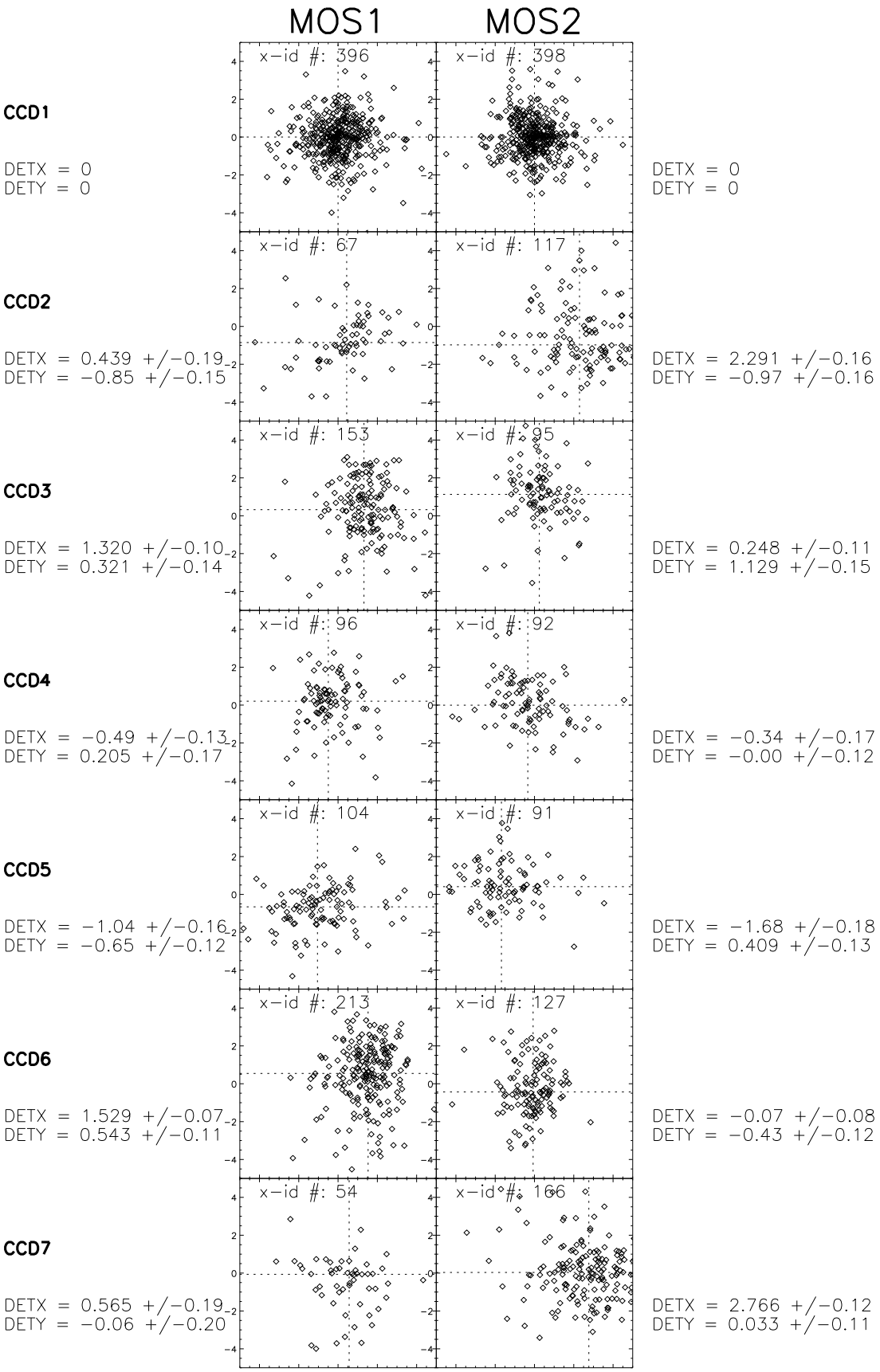

Figure 1: MOS relative offsets with respect to central CCD of sources with their optical counterpart, in arcseconds, in camera coordinate axis for different CCDs, one point per source.

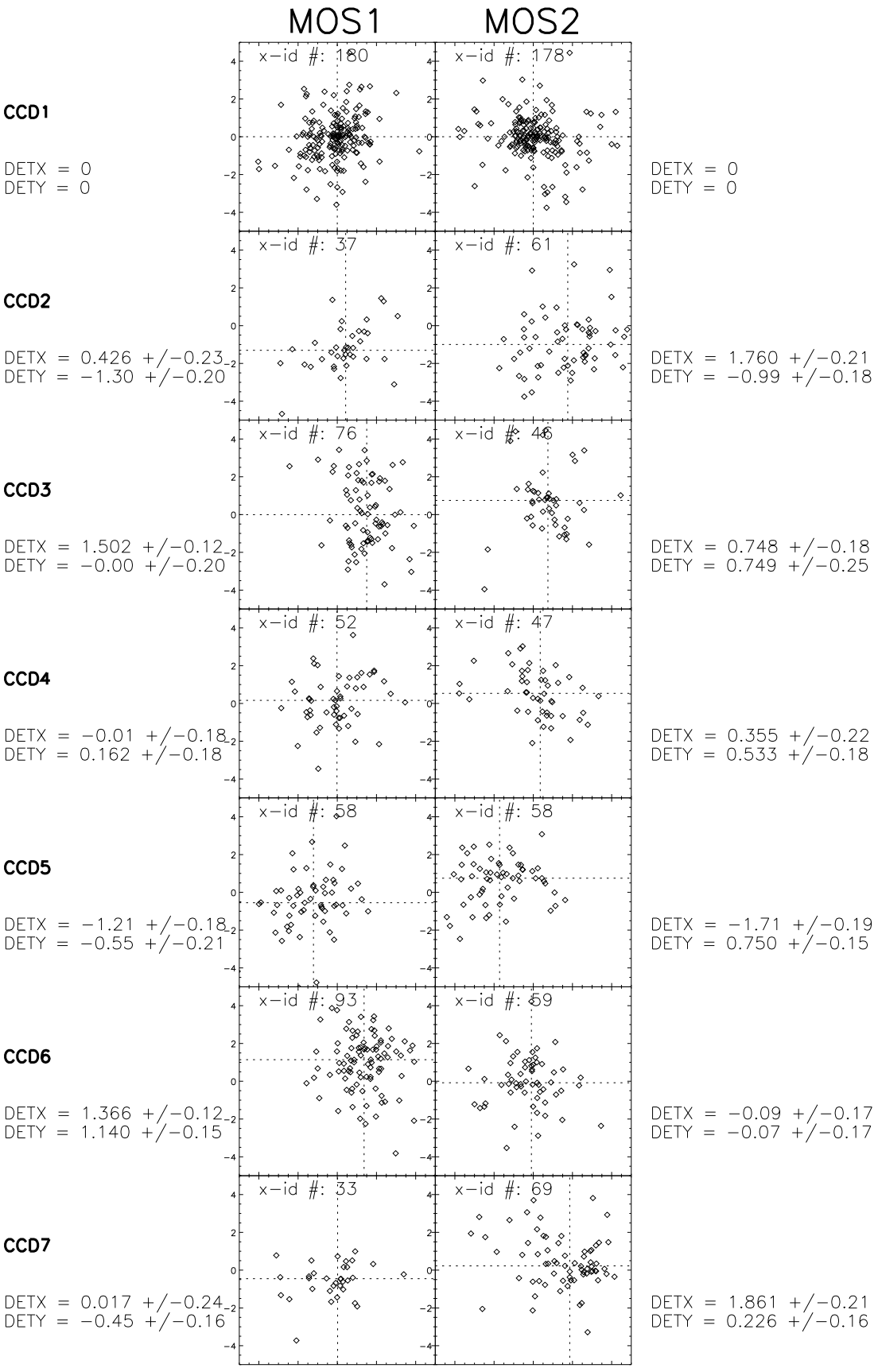

Figure 2: MOS relative offsets with respect to central CCD of sources with their EPIC-pn counterpart, in arcseconds, in camera coordinate axis for different CCDs, one point per source.

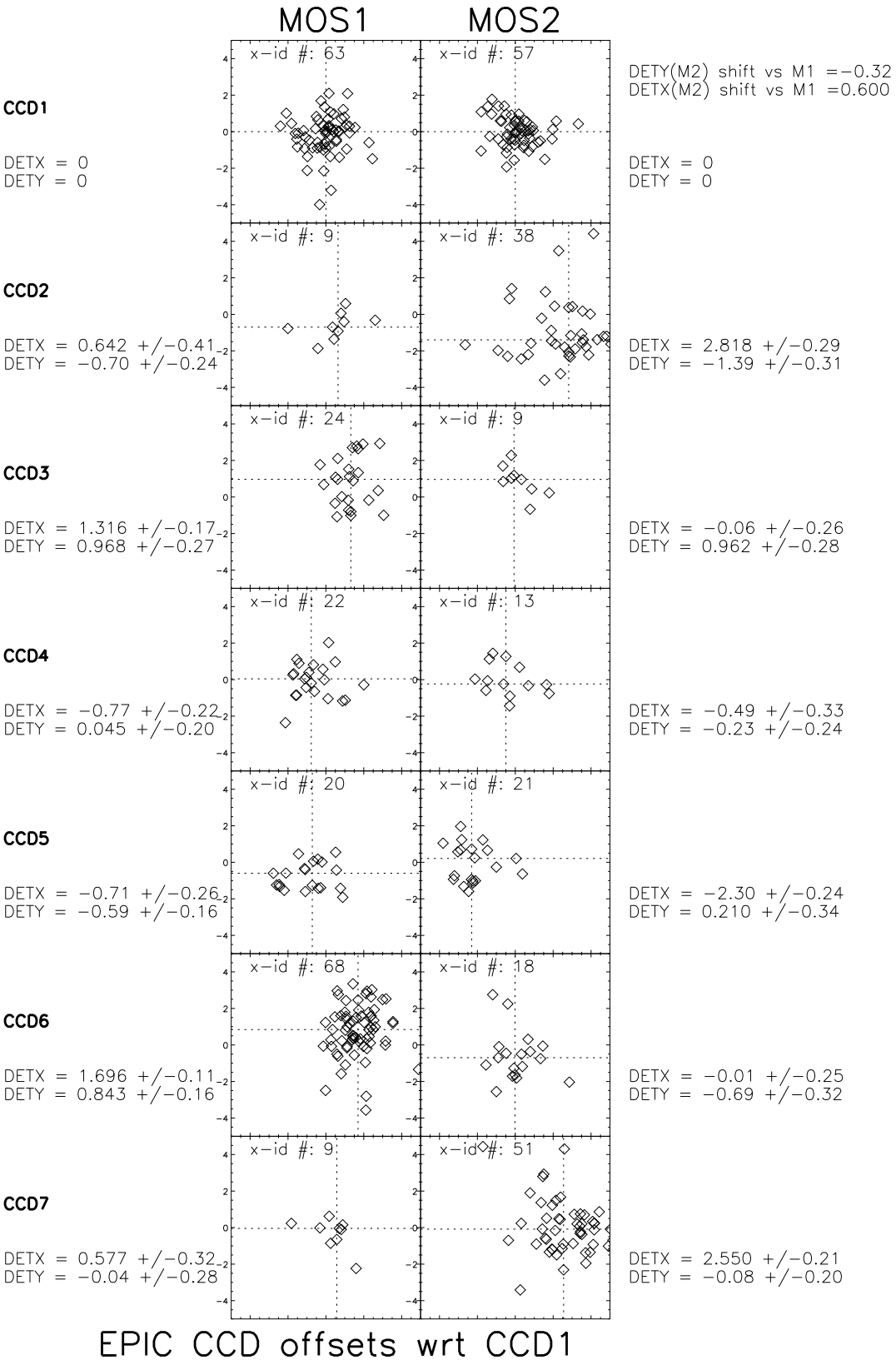

Figure 3: MOS relative offsets with respect to central CCD of sources with their optical counterpart, in arcseconds, in camera coordinate axis for different CCDs, for one field (OMC2/3) with the **old LINCOORD CCF 16**.

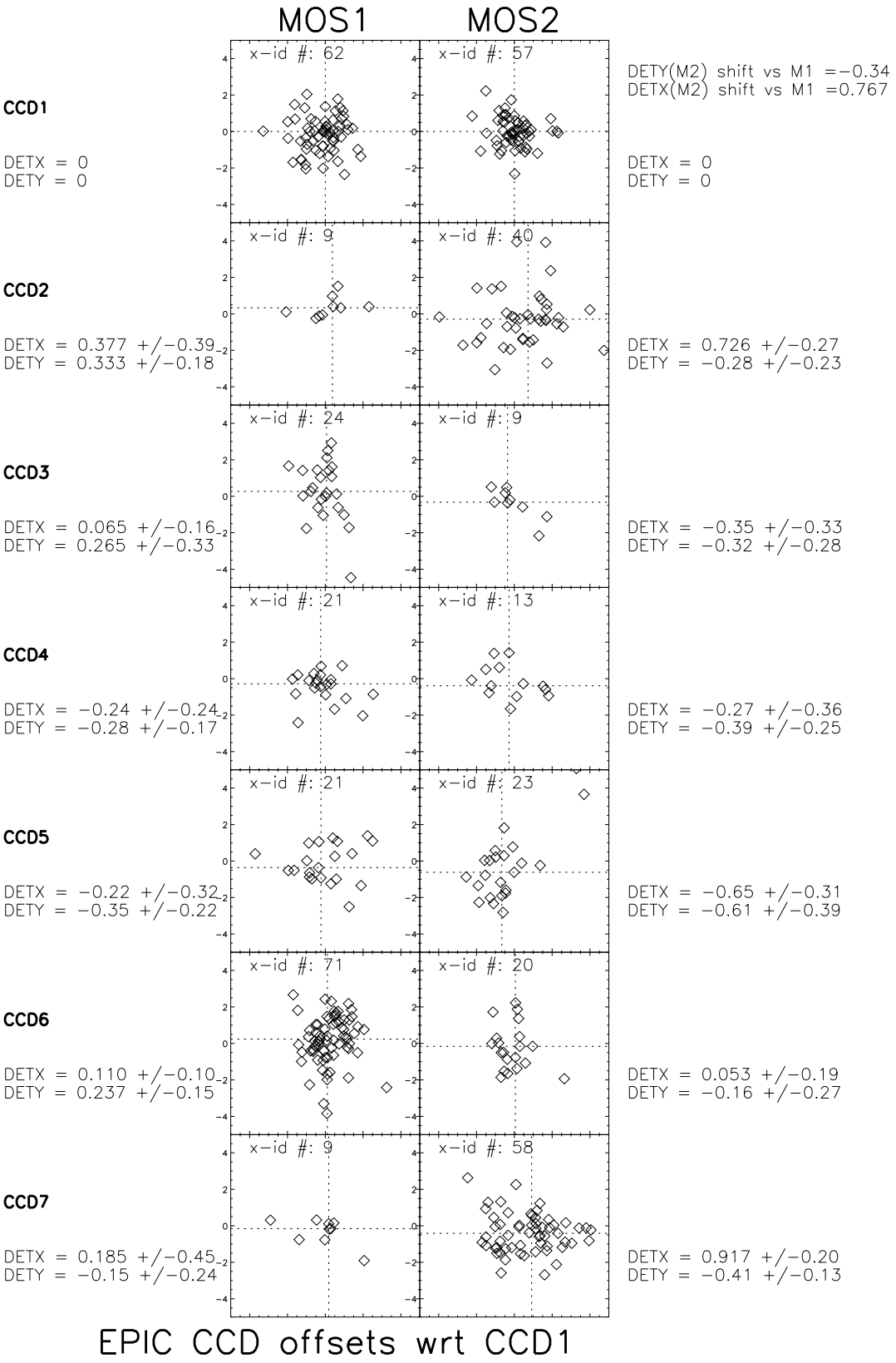

Figure 4: MOS relative offsets with respect to central CCD of sources with their optical counterpart, in arcseconds, in camera coordinate axis for different CCDs, for one field (OMC2/3) with the **new LINCCORD CCF 17**.

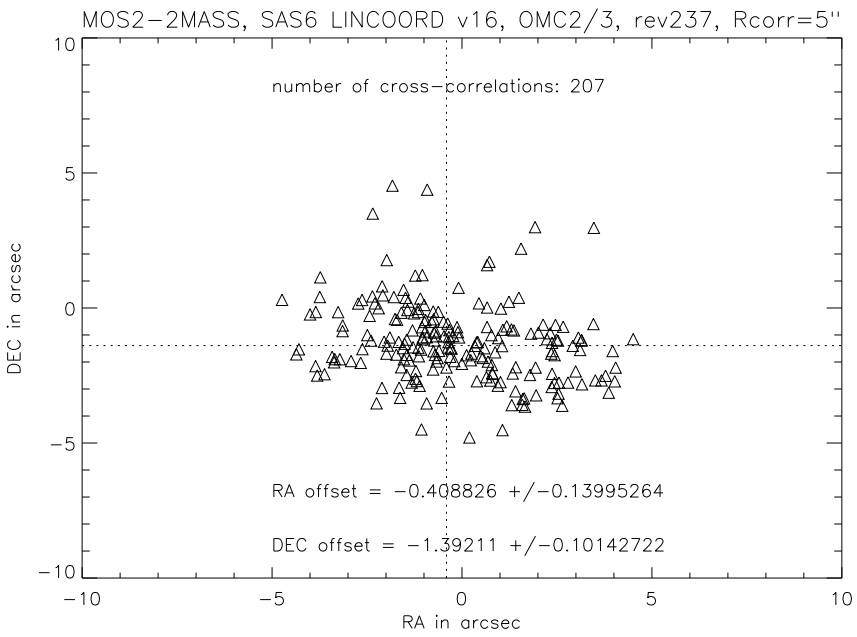

Figure 5: Scatter plot of the offsets with the optical positions for all MOS2 sources in the OMC2/3 field (rev237) in celestial coordinates, with the old LINCOORD CCF v16.

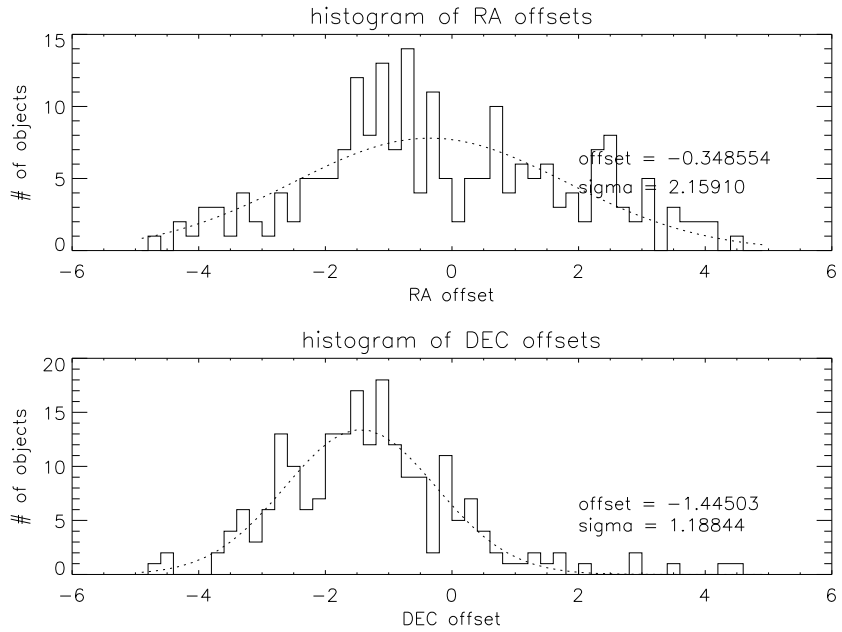

Figure 6: Histogram of the distribution of the RA and DEC sky position offsets with the optical for all MOS2 sources in the OMC2/3 field (rev237), with the nold LINCOORD CCF v16.

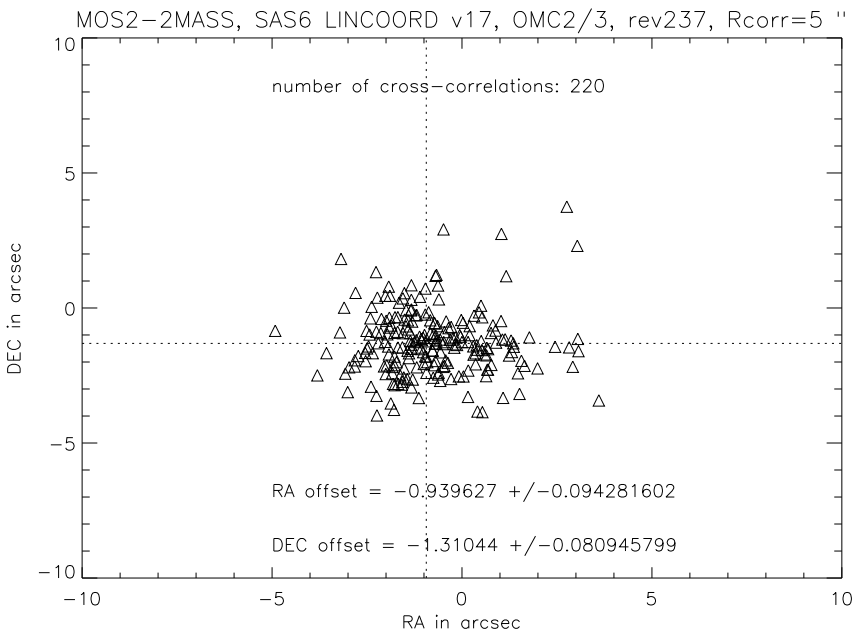

Figure 7: Scatter plot of the offsets with the optical positions for all MOS2 sources in the OMC2/3 field (rev237) in celestial coordinates, with the new LINCOORD CCF v17.

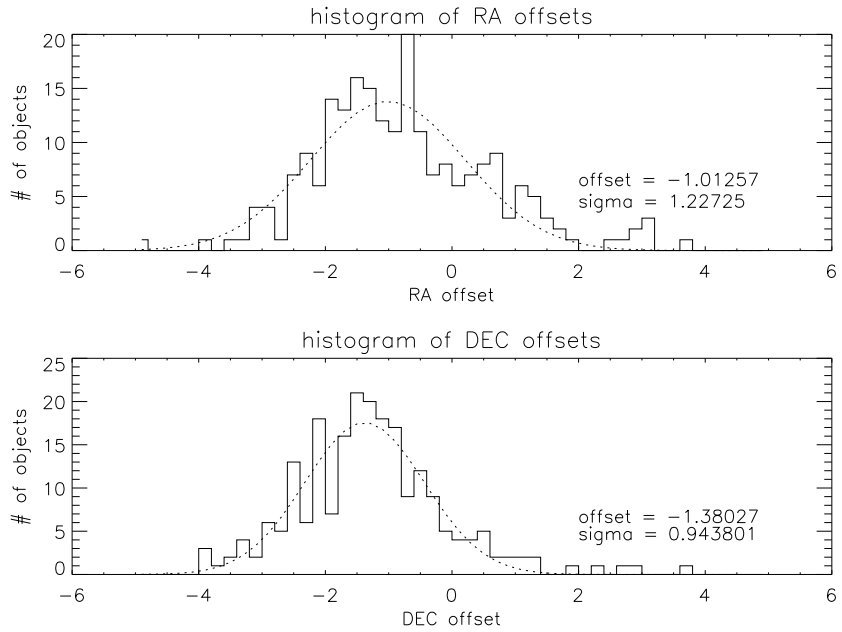

Figure 8: Histogram of the distribution of the RA and DEC sky position offsets with the optical for all MOS2 sources in the OMC2/3 field (rev237), with the new LINCOORD CCF v17.

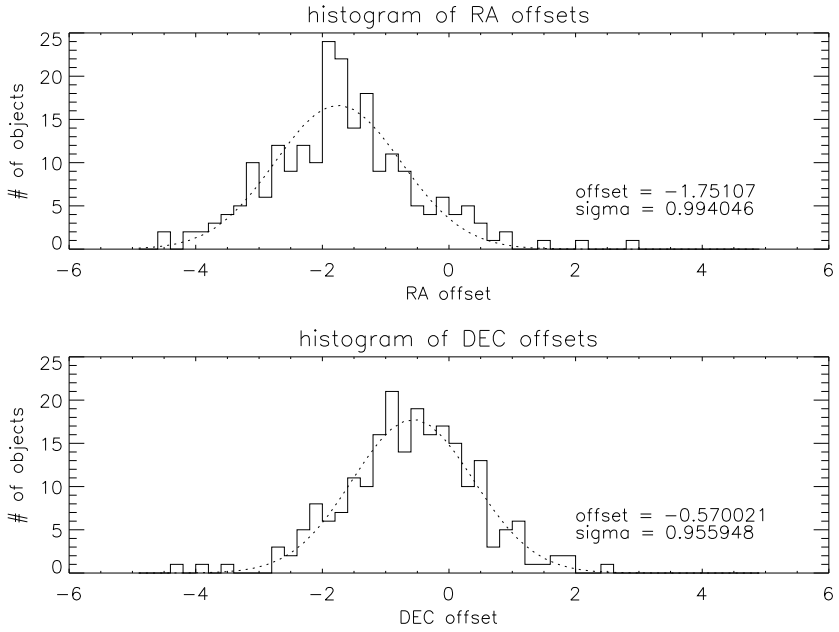

Figure 9: Histogram of the distribution of the RA and DEC sky position offsets with the optical for all MOS1 sources in the OMC2/3 field (rev237).

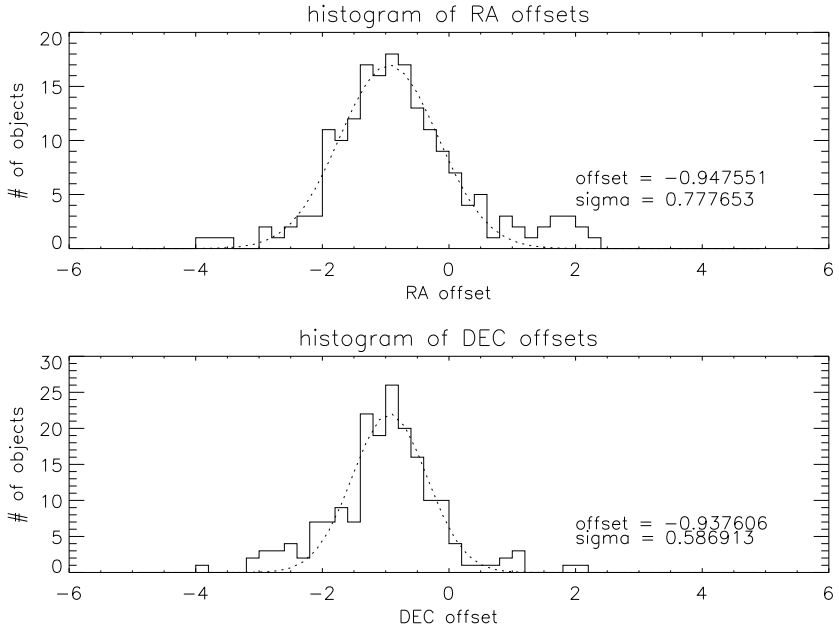

Figure 10: Histogram of the distribution of the RA and DEC sky position offsets with the optical for all EPIC-pn sources in the OMC2/3 field (rev237).